EBioMedicine 66 (2021) 103325

Contents lists available at ScienceDirect

EBioMedicine

journal homepage: www.elsevier.com/locate/ebiom

Research Paper

The transition from normal lung anatomy to minimal and established fibrosis in idiopathic pulmonary fibrosis (IPF)

Feng Xu[a], Naoya Tanabe[a,b], Dragos M. Vasilescu[a], John E. McDonough[c], Harvey C. Coxson[a], Kohei Ikezoe[a], Daisuke Kinose[a,d], Kevin W. Ng[e], Stijn E. Verleden[f], Wim A. Wuyts[c], Bart M. Vanaudenaerde[c], Johny Verschakelen[c], Joel D. Cooper[g], Marc E. Lenburg[h], Katrina B. Morshead[i], Alexander R. Abbas[i], Joseph R. Arron[i], Avrum Spira[h], Tillie-Louise Hackett[a], Thomas V. Colby[j], Christopher J. Ryerson[a,k], Raymond T. Ng[l], James C. Hogg[a,*]

[a] Center for Heart Lung Innovation, The University of British Columbia, Vancouver, Canada
[b] Department of Respiratory Medicine, Graduate School of Medicine, Kyoto University, Kyoto, Japan
[c] Leuven Lung Transplant Unit, KU Leuven and UZ Gasthuisberg, Leuven, Belgium
[d] Division of Respiratory Medicine, Department of Medicine, Shiga University of Medical Science, Shiga, Japan
[e] The Francis Crick Institute, London, UK
[f] Laboratory of Respiratory Diseases, BREATHE, Department of CHROMETA, KU Leuven, Leuven, Belgium
[g] Division of Thoracic Surgery, University of Pennsylvania, USA
[h] Boston University Medical Center, Boston, MA, USA
[i] Genentech, Inc., South San Francisco, CA, USA
[j] Department of Pathology and Laboratory Medicine, Mayo Clinic Arizona, USA
[k] Department of Medicine, The University of British Columbia, Vancouver, Canada
[l] Department of Computer Science, The University of British Columbia, Vancouver, Canada

ARTICLE INFO

Article History:
Received 16 January 2021
Revised 12 March 2021
Accepted 19 March 2021
Available online xxx

Keywords:
IPF
Integrative analysis
MDCT
Micro-CT
Quantitative histology
RNAseq

ABSTRACT

Background: The transition from normal lung anatomy to minimal and established fibrosis is an important feature of the pathology of idiopathic pulmonary fibrosis (IPF). The purpose of this report is to examine the molecular and cellular mechanisms associated with this transition.
Methods: Pre-operative thoracic Multidetector Computed Tomography (MDCT) scans of patients with severe IPF (n = 9) were used to identify regions of minimal(n = 27) and established fibrosis(n = 27). MDCT, Micro-CT, quantitative histology, and next-generation sequencing were used to compare 24 samples from donor controls (n = 4) to minimal and established fibrosis samples.
Findings: The present results extended earlier reports about the transition from normal lung anatomy to minimal and established fibrosis by showing that there are activations of *TGFBI, T* cell co-stimulatory genes, and the down-regulation of inhibitory immune-checkpoint genes compared to controls. The expression patterns of these genes indicated activation of a field immune response, which is further supported by the increased infiltration of inflammatory immune cells dominated by lymphocytes that are capable of forming lymphoid follicles. Moreover, fibrosis pathways, mucin secretion, surfactant, *TLRs*, and cytokine storm-related genes also participate in the transitions from normal lung anatomy to minimal and established fibrosis.
Interpretation: The transition from normal lung anatomy to minimal and established fibrosis is associated with genes that are involved in the tissue repair processes, the activation of immune responses as well as the increased infiltration of CD4, CD8, B cell lymphocytes, and macrophages. These molecular and cellular events correlate with the development of structural abnormality of IPF and probably contribute to its pathogenesis.

1. Introduction

The rapid decline in lung function with 50% mortality within 3–5 years of diagnosis of idiopathic pulmonary fibrosis (IPF) has defined the disease as one of the most devastating forms of

* Corresponding author.
E-mail address:

https://doi.org/10.1016/j.ebiom.2021.103325

Research in context

Evidence before this study

Based on a review of literature conducted in PubMed until Feb. 03, 2021, the number of terminal bronchioles has been reported to decrease during the pathogenesis of idiopathic pulmonary fibrosis (IPF) in only three publications [1–3]. However, little is known about the molecular and cellular mechanisms of the transition from normal lung anatomy to minimal and established fibrosis. We found no publication on the molecular and cellular events associated with IPF that are linked to concomitant structural and histological events as shown by MDCT, micro-CT, quantitative histology, and gene expression profiling.

Added value for this study

Based on gene expression profiling, the transition from normal lung anatomy to minimal and established fibrosis is associated with tissue repair genes, surfactant genes, TGFβ pathways, and pathways that could activate immune responses. The activation of immune responses in both minimal and established fibrosis is further supported by the increased infiltration of immune cells and the formation of non-encapsulated lymphoid follicles in IPF affected tissues. These molecular and cellular events are therefore likely triggers for the development of IPF.

Implication of all the available evidence

The results in this study substantially extend previous publications by providing new data on the molecular and cellular events associated with the transition from normal lung anatomy to minimal and established fibrosis. These events provide insights into how fibrosis in IPF is triggered. A better understanding of this mechanism could inform the discovery of potential therapeutic targets for IPF.

interstitial lung disease [4,5]. Anti-fibrotic therapies slow the rate of lung function decline in persons with IPF [6,7], but none of the currently available therapies consistently improve the quality of life associated with an established diagnosis of IPF. The incomplete effectiveness of these therapies is in part due to the unknown pathological mechanisms of fibrosis in IPF that limit the development of highly effective and targeted therapies. Thus, understanding the initial mechanisms of the disease is a crucial step towards identifying the underlying cause and possible therapeutic targets of IPF.

Recent studies had focused on genetic profiles using blood cells from different patients with IPF [8]. To date, these studies provide information on individual biopsy from a single point of time and require comparison from individuals with different genetic backgrounds and different stages of the disease. Further studies in which normal tissue samples are compared to diseased tissue of different severity obtained by random sampling of the whole lung are needed to address differences in structure, cellular and genetic changes on the same genetic background.

The purpose of this study is to investigate the gene expression profiles of the transition from normal lung anatomy to minimal and established fibrosis in IPF [1,2], using a novel method consisting of a combination of multidetector computed tomography (MDCT), micro-CT, quantitative histology, and gene expression profiling. The key genes and cells involved in these transitions have the potential to become novel therapeutic targets and/or biomarkers of this complicated disease.

2. Methods

2.1. Study design and participants

The diagnosis of IPF was made by a multidisciplinary consensus committee based on existing guidelines and confirmed by either pre-operative video-assisted thoracic surgical biopsy (VATS), or by pathological examination of the contralateral explanted lung specimens. In total, 9 IPF affected lungs and 4 donor control lungs provided a total of 78 (13×6) samples of lung tissue in this study. The demographic and clinical characteristics of both donor and IPF subjects are summarized in Table 1. The age, height, weight, sex ratio of the two groups were similar to each other. All patients with IPF were heavy smokers, while 3 out 4 controls were non-smokers.

2.2. Ethics

Informed consent for the study of explanted lungs was obtained directly from the patients with severe IPF before their treatment by lung transplantation and permission to study the donor lungs that served as controls was obtained either under Belgian law, where all eligible subjects automatically become donors or from the donor's next of kin in North America as described in detail by the gift of Life Donor Program (http://www.donors1.org). Data collection was approved by both the ethics (S52174) and biosafety (MS20101571) committees of the institution where the lung transplants were performed and shared through material transfer agreements among all of the institutions involved.

2.3. Pre-operative MDCT analyses

As part of the routine standard of care, pre-operative thoracic MDCT scans on all patients with severe IPF were taken with the following parameters: 1–5 mm slice thickness, 102–140 kV, and 80–140 mA. The diagnosis of minimal and established fibrosis was made by two experienced thoracic radiologists as previously described [1]. Following transplantation, explanted frozen lung specimens were scanned by MDCT with the following parameters: 1 mm slice thickness, 120 kV, 110 mA, reconstruction kernel 1.0 b60f on Siemens Somatom platform [1]. Results of the pre-operative thoracic MDCT scans of patients were registered onto the MDCT scans of their explanted lung specimens to facilitate the removal of samples from regions of minimal fibrosis (n = 27) and established fibrosis (n = 27).

2.4. Specimen preparation

The procedures used to prepare the explanted lung specimens in this project have been previously described in detail [9,10]. Briefly, each explanted lung specimen was inflated to total lung capacity with air and frozen solid in liquid nitrogen vapor. A multidetector computed tomography (MDCT) scan of the intact specimen was

Table 1
Demographic data

Variable\Group	IPF	Control
Patients No.	9	4
No. of samples	54	24
Age(years)	57 ± 5	56 ± 9
Height(cm)	172 ± 7	174 ± 7
Weight(kg)	72 ± 10	81 ± 17
Male:Female	9:0	4:0
Current: Never smoker	9:0	1:3

Six cores (1.4 cm in diameter and 2 cm in length) were collected from each explanted lung in this study.

obtained. The specimen was then kept frozen on dry ice while it was cut into 2 cm thick transverse slices using a band saw. Two cores (1.4 cm in diameter and 2 cm in length) in the upper, middle, and basal parts of the lung were selected (total 6 cores per lung) and stored at -80 °C. The frozen slice was photographed before and after tissue cores were obtained to identify the location of the lung samples.

2.5. Micro-CT analyses

Micro-CT of the selected cores was performed using a Bruker 1172 Skyscan micro-CT scanner at -30 °C at 7 9.9 μm resolution, followed by vacuum embedding of the frozen sample in optical cutting temperature compound for histological examination. The number of terminal bronchioles was counted using three-dimensional reconstructions of the micro-CT images [11]. Micro-CT images at 10 regular intervals along each tissue core were also used to measure the mean linear intercept (Lm) [12]. We chose to present the data of terminal bronchioles number/ unit surface area versus the mean linear intercept to demonstrate the relationship between the loss of surface area of the alveoli [LM] which is a marker of destruction by fibrosis and the loss of terminal bronchioles. The TB and Lm counts have previously been reported elsewhere [1].

2.6. Histological analyses

A quantitative histological analysis was performed on frozen sections cut from the same cores of lung tissue that were examined by micro-CT as previously described [1]. As an alternative to flow cytometry for quantitating individual cell types, we conducted immunohistochemistry staining and classical quantitative histological imaging [13–15] in our study. The technical details of immunohistochemistry staining and quantitative histological imaging in this study are well described in the previous publications [10,13–16]. The volume fractions of tissue containing tertiary lymphoid follicles, small airways, and parenchymal tissue staining positive for individual inflammatory cells, including CD4 T cells, CD8 T cells, polymorphonuclear neutrophils(PMN)[NP57], macrophages [CD68], *B* cells [CD79a], were all assessed in this study [10,13–16].

2.7. Gene expression profiles analyses

Qiagen RNeasy columns were used to extract the RNA from all samples. miRNA and non-human RNA were removed during library preparation. The sequencing library was prepared utilizing Illumina Truseq. All of the 78 samples were then sequenced on the Illumina HiSeq 2500 platform as 50 bp single-end reads. Reads were aligned to the NCBI human reference genome (Build 38) using GSNAP v.2013- 10-10, allowing a maximum of two mismatches per 50-base sequence. Gene expression levels were calculated as normalized RPKM from the number of reads mapped to the exons of each RefSeq gene using the functionality provided by the *R*/Bioconductor package GenomicAlignments. The RPKM (reads per kilobase of transcript, per million mapped reads) was further converted to TPM (transcripts per million) for the downstream analysis. The gene expression data has been uploaded to the European Genome-phenome Archive (EGA) and is available under the accession EGAS00001004758.

2.8. Statistical analyses

Gene expression data from the RNA sequencing were subjected to statistical analyses as follows:

1. Statistical analyses were performed using the *R* program (version 3.5.0). Differential expression genes were identified on the basis of the linear mixed effect model (LMM) as follows:

$$\begin{aligned} &\mathrm{Gene}_{ij} = \beta_0 + \beta_{\mathrm{Group}} \times \mathrm{Group}_{ij} + \alpha_j + \varepsilon_{ij} \\ &\varepsilon_{ij} \sim N(0, \sigma^2), \quad \alpha_j \sim N\left(0, \sigma^2_{a_j}\right), \quad i = 1,\ 2,\ \ldots,\ 6; \quad j = 1,\ 2,\ \ldots 13 \end{aligned} \tag{1}$$

In Eq. (1), *j* is the index for the explanted lungs, while *i* is the index for the samples in the corresponding lung. Gene_{ij} is the expression levels of distinct genes in each core from different lungs. Group_{ij} is the fixed term represents the group information of each core, including control, minimal fibrosis, and established fibrosis categories. β_{Group} is the coefficient of Group_{ij} term. The random effect term α_j represents the random effect of different patients. α_j is assumed to follow the 0 mean and $\sigma^2_{a_j}$ variance normal distribution, which is used to adjust the effect of multiple samples from the same explanted lungs. The random term ε_{ij} is the random error, which follows the Gaussian distribution of 0 mean and σ^2 variance. β_0 is the intercept of the model. The false discovery rate (FDR) < 0.1, which illustrate the fitting quality of β_{Group}, was used to identify the differential expressed genes in minimal fibrosis, established fibrosis, and all IPF samples. The differences in terminal bronchiole number, Lm value, the infiltration of different immune cells among distinct groups were also tested by the similar linear mixed effect model (LMM). The stability of the linear mixed effect model has been double tested (More details in Online Supplementary Methods and Supplementary Table 1). Besides the differential expressed genes identified by LMM, we further noted that some genes, whose FDR was just beyond the 0.1 cutoffs, had very big β_{Group} coefficient. To further study these genes with big β_{Group} coefficient, post-hoc, fold change and Mann–Whitney–Wilcoxon tests were used to further explore the expression of these genes (More details in Online Supplementary Methods). Cohen's *d* value was used to estimate the effect size in this study [17].

2. Gene Set Enrichment Analysis (GSEA) was utilized to explore the differentially expressed genes according to functional pathways such as coagulation and epithelial mesenchymal transition in minimal fibrosis, established fibrosis, and all IPF samples [18].

2.9. Role of funding source

The funding source, namely Canadian Institute of Health Research, BC Lung Association, Katholieke Universiteit Leuven, and Genentech, had neither a role in the study design, data collection, analyses, or data interpretation nor in the drafting of this paper. The mRNA levels in this study are profiled by Genentech. The corresponding author, Dr. James C. Hogg, had full access to all the data in the study and had final responsibility for the decision to submit the project.

3. Results

3.1. Micro-CT findings

Micro-CT results showed a marked decrease in the number of terminal bronchioles in both the minimal and established fibrotic regions of the IPF lungs compared to donor control lungs (Fig. 1a, p-value $< 1.6 \times 10^{-8}$). The change in Lm (loss of surface area) between the control and regions of minimal fibrosis was not significantly different (Fig. 1a, p-value < 0.27) but, the Lm in regions of established fibrosis increased significantly compared with control (Fig. 1a, p-value $< 6.8 \times 10^{-6}$). Fig. 1a demonstrates the relationship between the loss of surface area of the alveoli [Lm] which is a marker of destruction by fibrosis and the loss of terminal bronchioles. An increase in fibrous connective tissues was observed in the interstitial space in the regions of minimal and established fibrosis (Fig. 1b–d).

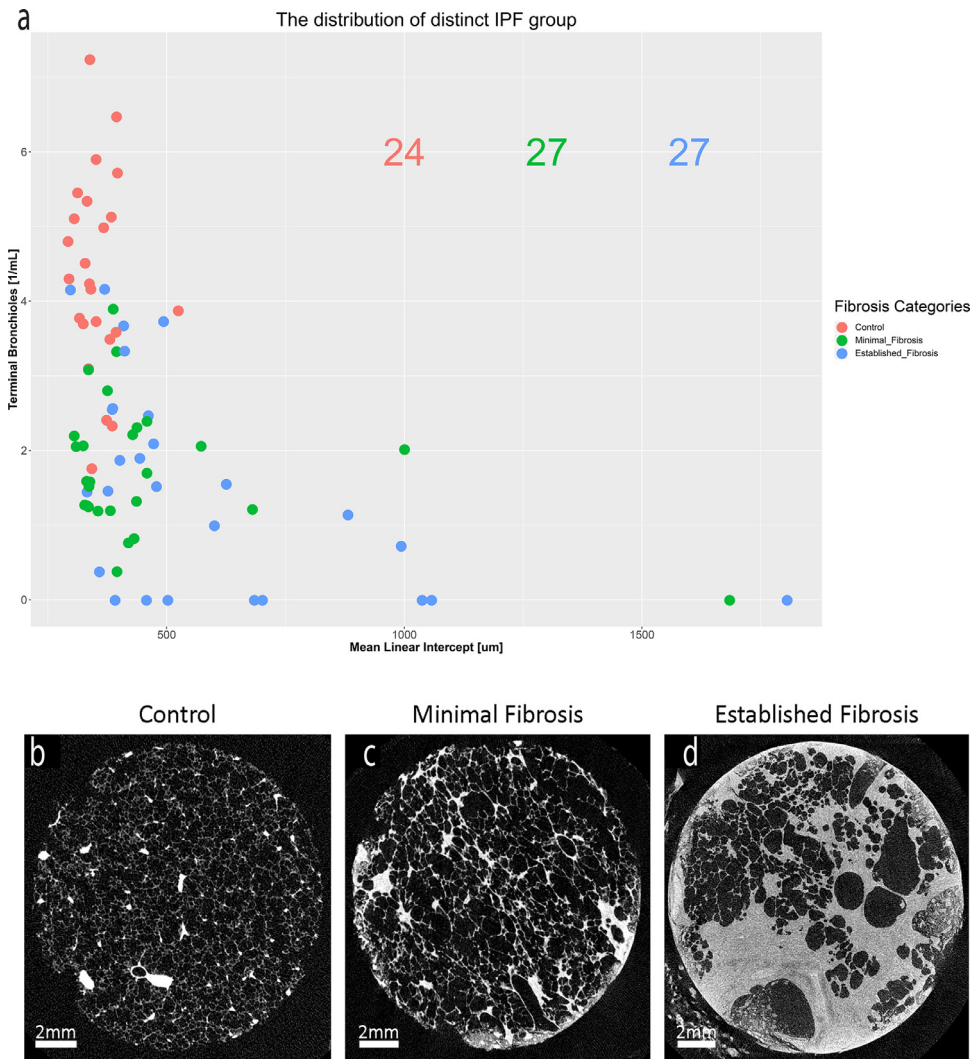

Fig. 1. The decrease of terminal bronchioles number and increase of mean linear intercept (Lm) in fibrosis samples—results from micro-CT analyses.

The mean linear intercept (Lm) is a morphometric estimate of alveolar surface destruction: an increase in Lm indicates a decrease in lung surface area, a marker of fibrosis. Additional details of the calculation of the mean linear intercept are shown in full in the online supplementary file. Panel (a) The number of terminal bronchioles/ml lungs decrease in both minimal (p-value $< 1.6e^{-8}$) and established fibrosis regions (p-value $< 1.3e^{-7}$). Panel (b) shows a micro-CT image of a control sample. Panel (c) and (d) show the micro-CT images of two IPF lung samples with minimal fibrosis and established fibrosis, respectively. Airspace enlargement and fiber accumulation could be observed in both minimal and established fibrosis samples.

3.2. Histological findings

We found greater infiltration of CD4 *T* cells, CD8 *T* cells, *B* cells, and macrophages in minimal and established fibrosis when compared with controls (Fig. 2a–d). Tertiary lymphoid follicles which document the presence of a field immune response, in both minimal and established fibrosis, support the presence of an active adaptive immune response (Supplementary Fig. 1). There was no difference in the infiltration levels of neutrophils across disease states (Fig. 2e).

3.3. Gene expression analyses findings

Overall, we identified 523 up-regulated genes and 421 down-regulated in regions of minimal fibrosis compared to control lungs (Supplementary Fig. 2a & b). The number of up-regulated genes for established fibrosis and all IPF samples were 2089 and 986, respectively, while the numbers of down-regulated genes were 1666 and 998, respectively (Supplementary Fig. 2c).

The Gene Set Enrichment Analysis (GSEA) [18] further showed differential expression by pathways. Some genes that were up-regulated in fibrosis samples, such as *MMP7, TNF*, and *PLAU*, were genes involved in the tissue repair process (Fig. 3a). The GSEA also identified a group of 'gene lists', such as "Epithelial Mesenchymal Transition (EMT)" and "Coagulation" in IPF up-regulated & down-regulated genes (Supplementary Fig. 3a & 3b). *TGFBI*, a gene that is known to participate in the EMT process, is up-regulated in fibrosis (Fig. 3b, p-value < 0.001, effect size = 3.19). Genes involved in coagulation, such as *MMP7* and *MMP11*, as well as genes involved in EMT, such as *COL3A1, COL1A1*, and *ADAM12* were also up-regulated (Supplementary Fig. 4a–e, p-value < 0.001, *MMP7* effect size = 1.32, *MMP11* effect size = 1.64, *COL3A1* effect size = 1.78, *COL1A1* effect size = 1.80, *ADAM12* effect size = 2.31).

3.4.1. Activation of immune co-stimulatory markers & down-regulation of co-inhibitory receptors

CD28 and *CD86* were up-regulated (Fig. 4a,b, $p < 0.001$, *CD28* effect size = 1.41, *CD86* effect size = 1.18), and *CD274* (encoding the co-inhibitory receptor *PD-L1*) were down-regulated in both minimal and established fibrosis (Fig. 4c, $p < 0.05$, effect size = 1.46).

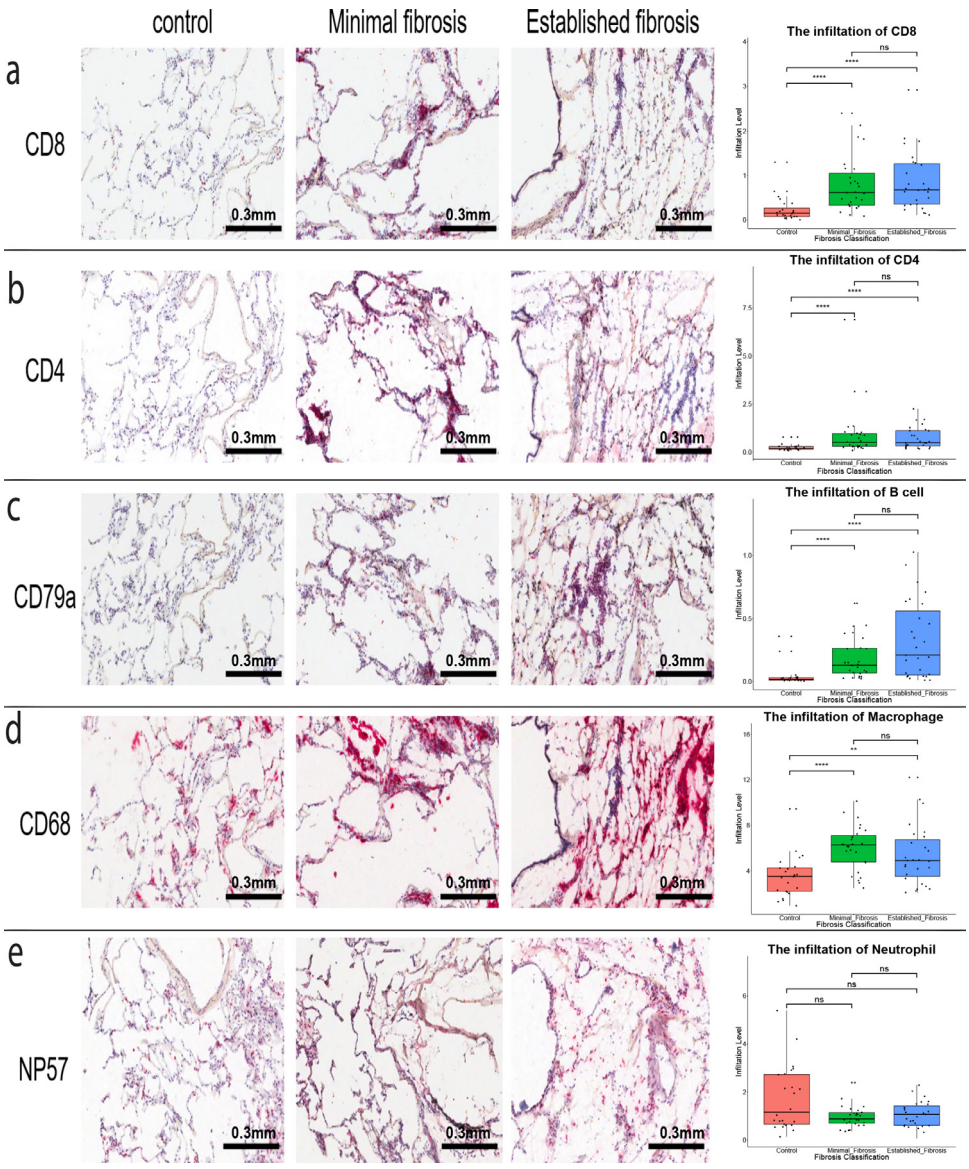

Fig. 2. Histological data in control and IPF samples.

The relationship between immune cell infiltration level [volume fractions of tissue positive on immunohistochemical staining for infiltrating cells] and the progression of fibrosis. The infiltration of CD8 *T* cell, CD4 *T* cell, *B* cell, macrophages, are significantly increased in minimal and established fibrosis[a–d, respectively]. Neutrophils did not show significant change across distinct fibrosis categories. *P*-value is calculated utilizing the linear mixed effect model. *:$p < 0.05$,**:$p < 0.01$, ***:$p < 0.005$, ****:$p < 0.001$.

3.4.2. *Pro-inflammatory signaling from toll-like receptors*

Besides the differential expressed genes identified by LMM, some of the genes, which has LMM FDR close to the cutoff 0.1, also had large β_{Group} coefficient, such as Toll-like receptors (TLRs) and hence their downstream targets subjected to post-hoc analyses using fold change and Mann-Whitney tests. As shown in Fig. 5a, TLRs can activate NFκB signaling pathway, which activates and propagate inflammatory genes and further immune responses. In our IPF samples, TLRs that could recognize both bacteria (*TLR4* and *TLR6*) and viruses (*TLR7* and *TLR8*) were significantly up-regulated (Fig. 5b–e, $p < 0.05$, *TLR4* effect size = 1.04, *TLR6* effect size = 1.20, *TLR7* effect size = 1.63, *TLR8* effect size = 1.53). Of the remainder of the TLRs, only *TLR2* was down-regulated (Supplementary Fig. 5a), and almost all other TLRs were up-regulated (Supplementary Fig. 5b–d). Their downstream targets, including components of the NFκB pathway, such as *NFKB1, TRAF3, PKD1*, and *CYLD*, were also up-regulated in the IPF samples (Fig. 5f, and Supplementary Fig. 6a–c).

3.4.3. *The expression patterns of other known IPF-related genes*

The expression of *MUC5B* (LMM output), which triggers the mucin secretion in IPF [19,20], was increased in both minimal and established fibrosis regions (Supplementary Fig. 7, *p*-value < 0.01, effect size = 0.56). Surfactant *C* and surfactant *D* were down-regulated, especially in the established fibrosis samples (Supplementary Fig. 8a–b, *p*-value < 0.01, *SFTPC* effect size = 0.64, *SFTPD* effect size = 0.50). Important transforming growth factors, namely *TGFB1, TGFB2*, and *TGFB3* and their receptor *TGFBR1*, were all up-regulated starting from the minimal fibrosis (Supplementary Fig. 9a–d, *p*-value < 0.001, *TGFB1* effect size = 1.65, *TGFB2* effect size = 1.56, *TGFB3* effect size = 1.22, *TGFBR1* effect size = 1.04). Additionally, *CASP1, NLRC4*, which participate in the activation of a cytokine storm [21,22], were all up-regulated in minimal fibrosis, while another cytokine storm trigger, *IL18* [23], was up-regulated in both minimal and established fibrosis regions (Supplementary Fig. 10a–c, *p*-value < 0.001, *CASP1* effect size = 0.97, *NLRC4* effect size = 1.48, *IL18* effect size = 1.56).

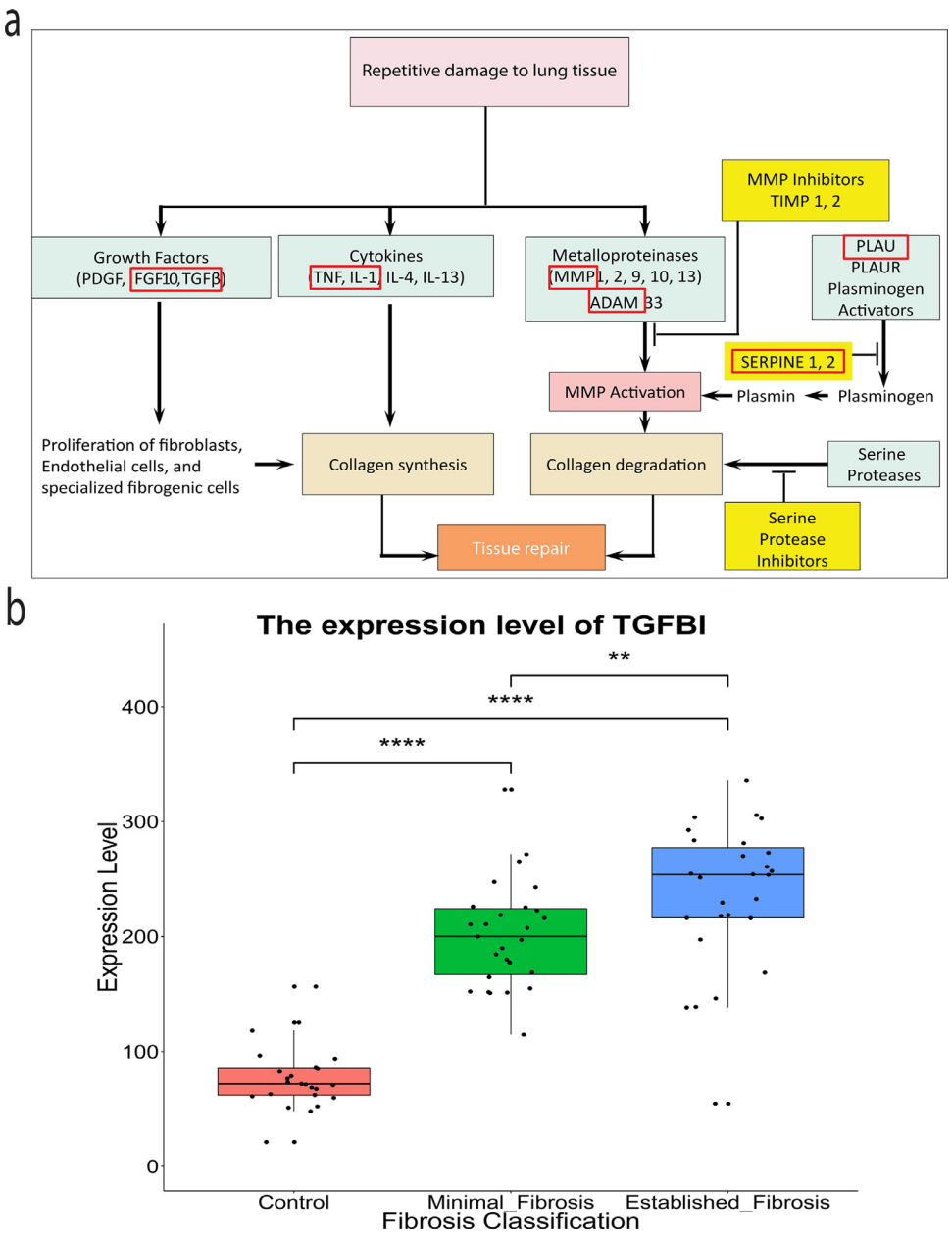

Fig. 3. The fibrosis-related differential expressed genes that participate in the repair of repetitively damaged tissue.

(a) The up-regulated fibrosis genes (genes in the red boxes: FGF10, TGFB, TNF, IL-1, MMP, ADAM33, PLAU, SERPINE 1 and 2) that are involved in the repetitive tissue repair procedure. The fibrosis genes in the red boxes are up-regulated in minimal and established fibrosis samples. This diagram is redrawn based on a previously reported overview of the genes involved in the repair of repetitively damaged tissue. (More details in the online supplement). **(b)** The expression level of TGFBI, which is involved in the epithelial mesenchymal transition, in three categories. P-value is calculated utilizing the linear mixed effect model. *:$p < 0.05$,**:$p < 0.01$, ***:$p < 0.005$, ****:$p < 0.001$.

4. Discussion

This study provides simultaneous evidence of structural, histological, immunological, and gene expression changes occurring in the transition from normal tissue to regions of minimal and established fibrosis in lungs with idiopathic pulmonary fibrosis. This study identifies many genetic pathways that are involved in the development and progression of IPF: pathways related to coagulation, epithelial mesenchymal transition, cellular immune responses, bacterial and viral defense, surfactant and mucous regulation, and cytokine storm production in addition to those of immune activation, repetitive tissue repair processes, and fibrosis. These events occurred against a background of increased infiltration of tissues by immune cells and structural loss of airways and alveolar wall destruction. To our knowledge this is the first study that has linked simultaneous molecular and cellular events indicating immune activation and tissue repair processes with different grades of structural abnormality in the same tissue in human lungs with IPF, thus providing direct evidence of linked key events in the pathogenesis of IPF.

Over-activation of the immune response could lead to the destruction of the lungs [24]. In this study, data on gene expression profiling show that over-activation of the genes related to immune responses could contribute to lung tissue damage observed in IPF, demonstrated by the concurrent findings of structural changes of the destruction of terminal bronchioles, and increased infiltration of immune cells and the formation of lymphoid follicles in regions of both minimal and established fibrosis. These results confirm and substantially extend earlier reports based on isolated cells from peripheral blood and bronchoalveolar lavage and tissue biopsy from patients with IPF and provided a novel, multidimensional cascade

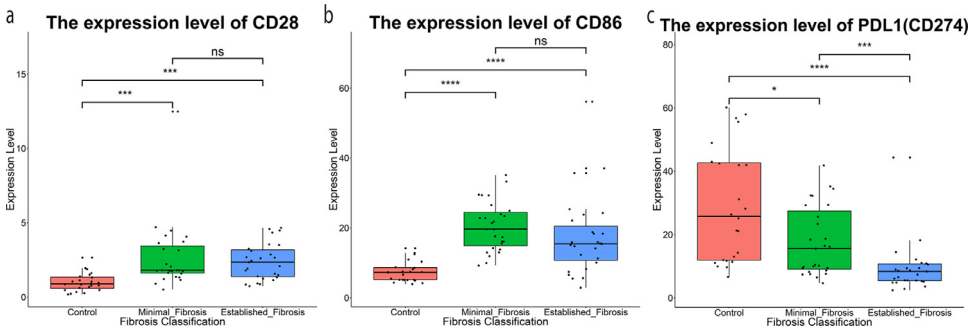

Fig. 4. The expression patterns of immune checkpoints genes.

The co-stimulatory immune checkpoint genes, namely *CD28* **(a)**, *CD86* **(b)**, are up-regulated in both minimal and established fibrosis. The inhibitory immune checkpoint gene, *PDL1(CD274)* **(c)**, is significantly down-regulated in fibrosis samples. These expression patterns support our hypothesis of immune response activation in IPF. P-value is calculated utilizing the linear mixed effect model. *:$p < 0.05$,**:$p < 0.01$, ***:$p < 0.005$, ****:$p < 0.001$.

that links clinical, MDCT, microCT, histology, and gene expression profiling to study IPF lung disease in order to provide linked information relevant to future treatment decisions.

Based on the expression patterns of immune checkpoint genes [regulation of T cells] and the presence of tertiary lymphoid follicles found in this study, we speculate that the smaller bronchi and bronchioles were destroyed by the activation of a field immune response [25], which damaged the lung tissue and led to the remodeling of both the airways and parenchyma. In support of this, we also identified a group of tissue repair genes, such as FGF10, TGFB, TNF, that are known to participate in immune response activation and tissue repair processes [26]. Based on the expression patterns of these tissue repair genes, we further postulate that the contraction of the connective tissue matrix, which is associated with wound healing, would destroy the structure of terminal bronchioles [27].

Small airways were lost in IPF in this study. In order to identify potential biomarkers for the destruction of terminal bronchioles in fibrosis, we compared the gene expression profiles of lung tissue with minimal fibrosis, established fibrosis, and controls. GSEA results showed that fibrosis up-regulated genes were enriched in "Coagulation" (e.g. *MMP7, MMP11*) and "Epithelial mesenchymal transition (EMT)" (e.g. *COL3A1, TGFBI*) pathways [18]. These findings are relevant in the pathogenesis of IPF as the coagulation pathway is involved in tissue repair and inflammation in IPF affected lungs [28] and EMT, during which epithelial cells gain the mesenchymal traits of invasion and migration, could trigger IPF [29]. Further, our finding of a marked up-regulation of TGFBI which can bind to collagen type I, II, IV, and affect fibrosis is also involved in EMT [30], and is a potential biomarker for the progression of IPF.

In this study, we found that toll-like receptors [TLRs] that could recognize both bacteria (*TLR4, TLR6, etc.*) and viruses (*TLR7, TLR8, etc.*) were significantly up-regulated and underscores the importance of infective exacerbations in the progression of IPF [5]. Although the up-regulation of TLR2 and TLR9 have been reported in bronchoalveolar lavage data and peripheral blood [31,32], our results show that TLRs are also up-regulated in whole lung tissue. Activation of TLRs could also contribute to wound healing and organ fibrosis [33] and result in downstream inflammatory signaling via NFκB signaling pathways. Indeed, our data showed that components of the NFκB pathway, including *NFKB1, TRAF3, PDK1*, and *CYLD*, were all up-regulated in fibrosis samples. The up-regulation of TLRs, as well as these pro-inflammatory genes, support our hypothesis that the immune response is activated in the lungs of IPF patients.

The activation of the immune response in IPF is further supported by the finding of increased expression of immune checkpoints genes, cytokine storm-related genes, and increased infiltration of inflammatory immune cells. Our analysis found several important pro-inflammatory genes, including *CD28, CD86* [34], that were up-regulated in fibrotic regions. Conversely, the inhibitory immune checkpoint gene, *CD274 (PDL1)* [35], was significantly down-regulated. Moreover, *CASP1, IL18, NLRC4*, which could initiate a cytokine storm and pro-inflammatory signaling through independent pathways [21,22], were all up-regulated in the minimal fibrosis samples. The activation of a cytokine storm might be responsible for the diffuse alveolar damage that could progress to minimal and established fibrosis [1,36]. Further, our histological analyses had found increased infiltration of immune cells and the formation of lymphoid follicles in both minimal and established fibrosis regions [1]. Although Adegunsoye et al. reported the increased infiltration of CD4+ *T* cells in lung biopsy [37], our study not only demonstrates the increased infiltration of CD4 T cells, we further provide evidence of infiltration of CD8 *T* cells, Macrophages, and *B* cells in IPF. These observations again support the concept of activation of immune responses, leading to the destruction of both airways and parenchyma and subsequent tissue repair processes involving collagen and fiber accumulation, ultimately resulting in fibrosis in the lungs of IPF patients.

Previous studies reported that TGFβ pathways were dormant in normal lungs, but were activated during tissue repair [38], and that the TGFβ pathway was up-regulated during lung fibrosis [39,40]. Consistent with these reports, we found that important components of TGFβ pathways, including *TGFB1, TGFB2, TGFB3*, and *TGFBR1*, were all up-regulated in both minimal and established fibrosis [41]. Taken together, our observations support the existence of lung injury and the activation of immune responses as key mechanisms of fibrosis in the lungs of IPF patients.

Immunofluorescence had been used to identify the dominance of MUC5B expressed cells in honeycomb cysts [42] and the association between a MUC5B promoter variant and rheumatoid arthritis (RA)-associated interstitial lung disease had been identified using GWAS analysis of peripheral blood [43]. Moreover, MUC5B had been reported to down-regulate surfactant proteins and co-expressed with surfactant in human [44]. In our dataset, we identified the up-regulation of *MUC5B* and the down-regulation of both surfactant *C* and surfactant *D*, especially in the established fibrosis samples. The down-regulation of both surfactant *C* and surfactant *D* could explain the collapse of alveoli in the IPF lungs due to the increase of surface tension in alveoli. These genes, including *MUC5B, SFTPC*, and *SFTPD*, may be explored as potential therapeutic targets of IPF in future studies.

This study has limitations. First, the number of patients analyzed in this project is relatively small. However, as our study design is based on explanted lung specimens and lung transplantations are relatively rare, it is not practical to obtain a large dataset. We acknowledge that a larger validation dataset is needed to test our proposed relationships between immune response activation and the transition from normal lung anatomy to IPF. Second, since it is impossible

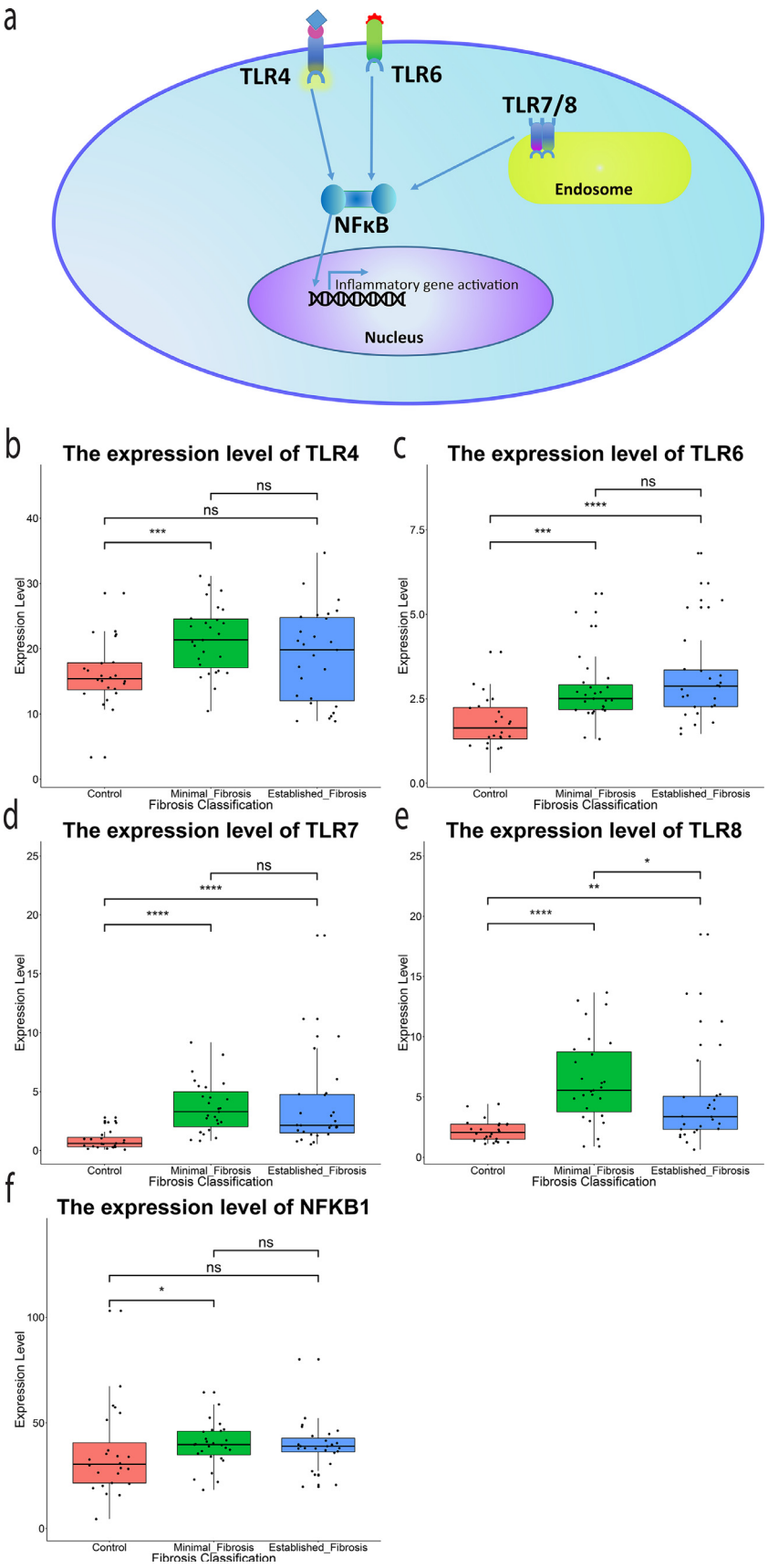

Fig. 5. Toll like receptors (TLRs) and its downstream targets.

(**a**) Schematic diagram of TLRs and their downstream targets. The gene expression of TLR4(**b**), TLR6(**c**), TLR7(**d**), TLR8(**e**), and NFκB1(**f**) in control, minimal fibrosis, and established fibrosis samples, respectively. *P*-value is calculated utilizing the linear mixed effect model. *:$p < 0.05$,**:$p < 0.01$, ***:$p < 0.005$, ****:$p < 0.001$.

to obtain a time series of lung samples, it is difficult for us to discriminate the initiation and progression of IPF. Moreover, it is hard to distinguish if an activated pathway is the real cause of the initiation or progression of the disease or just the responses to the development of the disease. However, we have attempted to do the next best thing by comparing normal lungs to diseased lungs with varying degrees of fibrosis based on the assumption that change from the normal lung to minimal and established fibrosis is associated over time. Third, the examination of mRNA levels reported in this study may not reflect actual up- or down-regulation of protein levels in the samples. However, the mRNA levels still offer strong evidence of the activation of the immune response during the transition from normal lung anatomy to both minimal and established fibrosis. Further, our histological experiments also support the activation of the immune response, which gives us confidence that these discoveries based on the mRNA expression levels are reliable. Fourth, although we identified the differential expression of genes and pathways in this report, these changes might be confounded by the infiltration of different immune cells. Further study on the single-cell level is needed to validate the gene expression pattern that we identified in this report. Lastly, although we found the molecular and cellular events associated with immune responses during the transition from normal lung anatomy to fibrosis, these findings could not be directly applied by the clinician. Further research, including but not limited to animal model tests, preclinical research, and clinical trials, is needed before these findings have direct clinical applications.

We would also like to emphasize the strengths of this study, which shows a novel and better method to study IPF lung disease compared to previous methods. Firstly, classic studies by Liebow and Carrington provided the classical pathology of IPF [45]. Recent studies had focused on genetic profiles using blood cells from different patients with IPF [8]. To date, these studies provide information on individual biopsy from a single point of time and require comparison from individuals with different genetic backgrounds and different stages of the disease. This study provides the opportunity to compare different regions of a lung with different grades of severity of disease on a single genetic background, thus removing inter-patients variability in the genetic background as a confounding variable in the comparison, and confirming the previous results in the intact lung. A second advantage lies in the unique design of the study, which makes it possible to link clinical lung imaging, microscopic structural changes shown by micro-CT, and quantitative histology to gene expression profiling within individual lungs. This integrative approach permitted the identification of changes in the transition from normal lung anatomy to minimal and established fibrosis. The third advantage of the study is the quality control of the study: (i) The grades of severity on clinical CT scans were independently scored by two experienced thoracic radiologists with resultant consensus; (ii) the histological grading of IPF was performed in two ways: initially score semiquantitatively by an experienced lung pathologist with a particular interest in IPF and then quantitatively by calculating the volume fractions of distinct immune cells in different compartments of the lungs with use of immunohistological staining.

In conclusion, the transition from normal lung anatomy to minimal and established fibrosis is a graded phenomenon and is associated with genes that are involved in the tissue repair processes, the activation of immune responses as well as the increased infiltration of CD4, CD8, *B* cell lymphocytes, and macrophages. These molecular and cellular events correlate with the development of structural abnormality of IPF and probably contribute to its pathogenesis.

Contributors

FX, NT, DMV, JEM, HCC, KI, DK, KWN, SEV, WAW, BMV, JV, MEL, AS, T-LH, TVC, CJR, RTN, and JCH analyzed, and interpreted the data. JEM, SEV, WAW, BMV, JV, JDC acquired and prepared the explanted lungs. KBM, ARA, JRA profiled the expression of the dataset. FX, NT, DMV, KWG, SEV, T-LH, RTN, and JCH conceived the study, delineated the hypothesis, and designed the study. FX and JCH drafted the manuscript. NT, DMV, HCC, KWN, SEV, T-LH, TVC, T-LH, CJR, and RTN revised and helped to improve the manuscript. All authors have read and approved the final version of the manuscript.

Declaration of Competing Interest

All other authors declare no competing interests.

Acknowledgments

The study was funded by Canadian Institute of Health Research (New investigator award), Katholieke Universiteit Leuven (C24/15/30 and C16/19/005), the BC Lung Association, and Genentech (Investigator award). The authors would like to thank all the donors who donated their explanted lungs to this study and the James Hogg Lung Registry (Darren Sutherland), Histology Core (Amrit Samra), and the Bio-Imaging Core (Aaron M Barlow) from the Centre for Heart Lung Innovation, St Paul's Hospital, Vancouver, BC, Canada. FX is supported by YS and Christable Lung Postgraduate Scholarship and IMS & NUS Allowance. NT has received grants from FUJIFILM, Dr. K.K Pump Fellowship of the BC Lung Association, and personal fees from Nippon Boehringer Ingelheim outside of the submitted work. DMV is supported by the Canadian Thoracic Society, Alpha-1 Foundation, and Parker B Francis fellowships. JEM is funded by the European Respiratory Society Respire. SEV is a senior research fellow of the Research Foundation Flanders (12G8715N, 1503620N, and G3C0494). T-LH is supported by the CIHR, Michael Smith Health Research Foundation, Parker B Francis, and Providence Health Care Research Institute New Investigator awards. JCH is funded by BC Lung association and Genentech Investigator Award.

Data sharing statement

The gene expression data has been uploaded to the European Genome-phenome Archive (EGA) under the accession EGAS00001004758. Qualified researchers could request access to anonymized individual patient-level data by sending a request to the corresponding author. Data will be shared after approval of a proposal, with a signed data access agreement.

Supplementary materials

Supplementary material associated with this article can be found in the online version at doi:10.1016/j.ebiom.2021.103325.

Reference

[1] Verleden SE, Tanabe N, McDonough JE, Vasilescu DM, Xu F, Wuyts WA, et al. Small airways pathology in idiopathic pulmonary fibrosis: a retrospective cohort study. Lancet Respir Med 2020;8(6):573–84.
[2] Tanabe N, McDonough JE, Vasilescu DM, Ikezoe K, Verleden SE, Xu F, et al. Pathology of idiopathic pulmonary fibrosis assessed by a combination of micro-computed tomography, histology, and immunohistochemistry. Am J Pathol 2020.
[3] Agarwal AK, Huda N. Interstitial pulmonary fibrosis. StatPearls. Treasure Island (FL) 2020.
[4] Raghu G, Remy-Jardin M, Myers JL, Richeldi L, Ryerson CJ, Lederer DJ, et al. Diagnosis of idiopathic pulmonary fibrosis. An official ATS/ERS/JRS/ALAT clinical practice guideline. Am J Respir Crit Care Med 2018;198(5):e44–68.
[5] Ley B, Collard HR, King TE. Clinical course and prediction of survival in idiopathic pulmonary fibrosis. Am J Respir Crit Care Med 2011;183(4):431–40.
[6] Noble PW, Albera C, Bradford WZ, Costabel U, Glassberg MK, Kardatzke D, et al. Pirfenidone in patients with idiopathic pulmonary fibrosis (CAPACITY): two randomised trials. Lancet 2011;377(9779):1760–9.
[7] Richeldi L, du Bois RM, Raghu G, Azuma A, Brown KK, Costabel U, et al. Efficacy and safety of nintedanib in idiopathic pulmonary fibrosis. N Engl J Med 2014;370(22):2071–82.

[8] Allen RJ, Guillen-Guio B, Oldham JM, Ma SF, Dressen A, Paynton ML, et al. Genome-wide association study of susceptibility to idiopathic pulmonary fibrosis. Am J Respir Crit Care Med 2020;201(5):564–74.
[9] Vasilescu DM, Phillion AB, Tanabe N, Kinose D, Paige DF, Kantrowitz JJ, et al. Non-destructive cryomicro-CT imaging enables structural and molecular analysis of human lung tissue. J Appl Physiol 2017;122(1):161–9 (1985).
[10] Vasilescu DM, Phillion AB, Kinose D, Verleden SE, Vanaudenaerde BM, Verleden GM, et al. Comprehensive stereological assessment of the human lung using multi-resolution computed tomography. J Appl Physiol 1985:2020.
[11] Tanabe N, Vasilescu DM, McDonough JE, Kinose D, Suzuki M, Cooper JD, et al. Micro-computed tomography comparison of preterminal bronchioles in centrilobular and panlobular emphysema. Am J Respir Crit Care Med 2017;195(5):630–8.
[12] Ashcroft T, Simpson JM, Timbrell V. Simple method of estimating severity of pulmonary fibrosis on a numerical scale. J Clin Pathol 1988;41(4):467–70.
[13] Howard MGR CV. Unbiased stereology: three-dimensional measurement in microscopy. BIOS Scientific Publishers Limited; 1998 Published in the US, its dependent territories and Canada1998.
[14] Weibel ER. Morphometry of the human-lung - state of the art after 2 decades. Bull Eur De Physiopathol Respir Clin Respir Physiol 1979;15(5):999–1013.
[15] Weibel ER. Morphometry of the human lung. New York: Academic Press Inc; 1963.
[16] Tanabe N, Vasilescu DM, Kirby M, Coxson HO, Verleden SE, Vanaudenaerde BM, et al. Analysis of airway pathology in COPD using a combination of computed tomography, micro-computed tomography and histology. Eur Respir J 2018;51(2).
[17] Sullivan GM, Feinn R. Using effect size-or why the P value is not enough. J Grad Med Educ 2012;4(3):279–82.
[18] Subramanian A, Tamayo P, Mootha VK, Mukherjee S, Ebert BL, Gillette MA, et al. Gene set enrichment analysis: a knowledge-based approach for interpreting genome-wide expression profiles. Proc Natl Acad Sci USA 2005;102(43):15545–50.
[19] Yang IV, Fingerlin TE, Evans CM, Schwarz MI, Schwartz DA. MUC5B and idiopathic pulmonary fibrosis. Ann Am Thorac Soc 2015;12(Suppl 2):S193–9.
[20] Zhang Y, Noth I, Garcia JG, Kaminski N. A variant in the promoter of MUC5B and idiopathic pulmonary fibrosis. New Engl J Med 2011;364(16):1576–7.
[21] Miao EA, Rajan JV, Aderem A. Caspase-1-induced pyroptotic cell death. Immunol Rev 2011;243(1):206–14.
[22] Suzuki T, Franchi L, Toma C, Ashida H, Ogawa M, Yoshikawa Y, et al. Differential regulation of caspase-1 activation, pyroptosis, and autophagy via Ipaf and ASC in Shigella-infected macrophages. PLoS Pathog 2007;3(8):e111.
[23] Davis BK, Wen H, Ting JP. The inflammasome NLRs in immunity, inflammation, and associated diseases. Annu Rev Immunol 2011;29:707–35.
[24] McDonough JE, Yuan R, Suzuki M, Seyednejad N, Elliott WM, Sanchez PG, et al. Small-airway obstruction and emphysema in chronic obstructive pulmonary disease. New Engl J Med 2011;365(17):1567–75.
[25] Iwasaki A, Foxman EF, Molony RD. Early local immune defences in the respiratory tract. Nat Rev Immunol 2017;17(1):7–20.
[26] Hogg JC, McDonough JE, Gosselink JV, Hayashi S. What drives the peripheral lung-remodeling process in chronic obstructive pulmonary disease? Proc Am Thorac Soc 2009;6(8):668–72.
[27] Wynn TA. Cellular and molecular mechanisms of fibrosis. J Pathol 2008;214 (2):199–210.
[28] Crooks MG, Hart SP. Coagulation and anticoagulation in idiopathic pulmonary fibrosis. Eur Respir Rev 2015;24(137):392–9.
[29] Jolly MK, Ward C, Eapen MS, Myers S, Hallgren O, Levine H, et al. Epithelial-mesenchymal transition, a spectrum of states: role in lung development, homeostasis, and disease. Dev Dyn 2018;247(3):346–58.
[30] Schwanekamp JA, Lorts A, Sargent MA, York AJ, Grimes KM, Fischesser DM, et al. TGFBI functions similar to periostin but is uniquely dispensable during cardiac injury. PloS One 2017;12(7):e0181945.
[31] Samara KD, Antoniou KM, Karagiannis K, Margaritopoulos G, Lasithiotaki I, Koutala E, et al. Expression profiles of toll-like receptors in non-small cell lung cancer and idiopathic pulmonary fibrosis. Int J Oncol 2012;40(5):1397–404.
[32] Huang Y, Ma SF, Espindola MS, Vij R, Oldham JM, Huffnagle GB, et al. Microbes are associated with host innate immune response in idiopathic pulmonary fibrosis. Am J Respir Crit Care Med 2017;196(2):208–19.
[33] Huebener P, Schwabe RF. Regulation of wound healing and organ fibrosis by toll-like receptors. Biochim Biophys Acta 2013;1832(7):1005–17.
[34] Camperio C, Muscolini M, Volpe E, Di Mitri D, Mechelli R, Buscarinu MC, et al. CD28 ligation in the absence of TCR stimulation up-regulates IL-17A and pro-inflammatory cytokines in relapsing-remitting multiple sclerosis T lymphocytes. Immunol Lett 2014;158(1-2):134–42.
[35] Darvin P, Toor SM, Sasidharan Nair V, Elkord E. Immune checkpoint inhibitors: recent progress and potential biomarkers. Exp Mol Med 2018;50(12):1–11.
[36] Coxson HO, Hogg JC, Mayo JR, Behzad H, Whittall KP, Schwartz DA, et al. Quantification of idiopathic pulmonary fibrosis using computed tomography and histology. Am J Respir Crit Care Med 1997;155(5):1649–56.
[37] Adegunsoye A, Hrusch CL, Bonham CA, Jaffery MR, Blaine KM, Sullivan M, et al. Skewed lung CCR4 to CCR6 CD4(+) T cell ratio in idiopathic pulmonary fibrosis is associated with pulmonary function. Front Immunol 2016;7:516.
[38] Selman M, Pardo A, Kaminski N. Idiopathic pulmonary fibrosis: aberrant recapitulation of developmental programs? PLoS Med 2008;5(3):e62.
[39] Hamanaka RB, O'Leary EM, Witt LJ, Tian Y, Gokalp GA, Meliton AY, et al. Glutamine metabolism is required for collagen protein synthesis in lung fibroblasts. Am J Respir Cell Mol Biol 2019.
[40] Chanda D, Otoupalova E, Smith SR, Volckaert T, De Langhe SP, Thannickal VJ. Developmental pathways in the pathogenesis of lung fibrosis. Mol Asp Med 2019;65:56–69.
[41] Kang H. Role of MicroRNAs in TGF-beta signaling pathway-mediated pulmonary fibrosis. Int J Mol Sci 2017;18(12).
[42] Seibold MA, Smith RW, Urbanek C, Groshong SD, Cosgrove GP, Brown KK, et al. The idiopathic pulmonary fibrosis honeycomb cyst contains a mucocilary pseudostratified epithelium. PLoS One 2013;8(3):e58658.
[43] Juge PA, Lee JS, Ebstein E, Furukawa H, Dobrinskikh E, Gazal S, et al. MUC5B promoter variant and rheumatoid arthritis with interstitial lung disease. N Engl J Med 2018;379(23):2209–19.
[44] Hancock LA, Hennessy CE, Solomon GM, Dobrinskikh E, Estrella A, Hara N, et al. Muc5b overexpression causes mucociliary dysfunction and enhances lung fibrosis in mice. Nat Commun 2018;9(1):5363.
[45] Liebow AA, Carrington CB. The interstitial pneumonias editor. In: Simon MPE, LeMay M, editors. Frontiers of pulmonary radiology. New York: Grune & Stratteon; 1969. p. 102–41.